JOURNAL OF THE STRUCTURAL DIVISION

TEST OF SCALE MODEL POST-TENSIONED FLAT PLATE

By Ned H. Burns,[1] M. ASCE and Roongroj Hemakom[2]

INTRODUCTION

Prestressed flat plates are widely used for multistory building construction, and they have performed well in service. However, more experimental data are needed to confirm the behavior of such slabs through the elastic and inelastic ranges and, finally, under collapse load. Some test data from complete structures (1,3,7,9) are available, but gaps still exist in verifying the minimum bonded steel requirement and shear strength. The isolated panel tests (4,5,8,11) were primarily aimed at determining shear strength of the slab and could not represent the actual slab behavior for the complete indeterminate structure. To confirm the reliability of the techniques of design and analysis which are in practical use, more experimental data for the total structural system are needed. The test of a structural concrete one-third scale "direct" model can simulate the behavior of the prototype both in elastic and inelastic range.

The primary objective of this investigation at The University of Texas, Austin, Tex., was to determine the physical behavior of the prestressed flat plate structure over the total range of loading up to the point of collapse. The investigation intended to answer some of the questions about distribution of cracking, the contribution of bonded reinforcement to strength, the stress increase in unbonded tendons with loading to ultimate, and the adequacy of present design methods. The safety of pre-stressed concrete slabs against punching shear failure was also investigated very closely. This paper describes the testing sequence and the observed behavior of the first model slab, Slab I, from a continuing study with two other model slabs (designated as Slab II and Slab III) which will be reported in a subsequent paper.

Note.—Discussion open until November 1, 1977. To extend the closing date one month, a written request must be filed with the Editor of Technical Publications, ASCE. This paper is part of the copyrighted Journal of the Structural Division, Proceedings of the American Society of Civil Engineers, Vol. 103, No. ST6, June, 1977. Manuscript was submitted for review for possible publication on July 22, 1976.

[1]Prof. of Civ. Engrg., Dept. of Civ. Engrg., The Univ. of Texas at Austin, Austin, Tex.

[2]Engr., Borton, Inc., Hutchinson, Kans.; formerly Research Asst., Dept. of Civ. Engrg., The University of Texas at Austin, Austin, Tex.

Description of Prototype Slabs and Test Structures

The prototype slab was designed as a floor in a typical medium-height apartment or office building with 30-ft (9-m) spans in each direction. The live load of

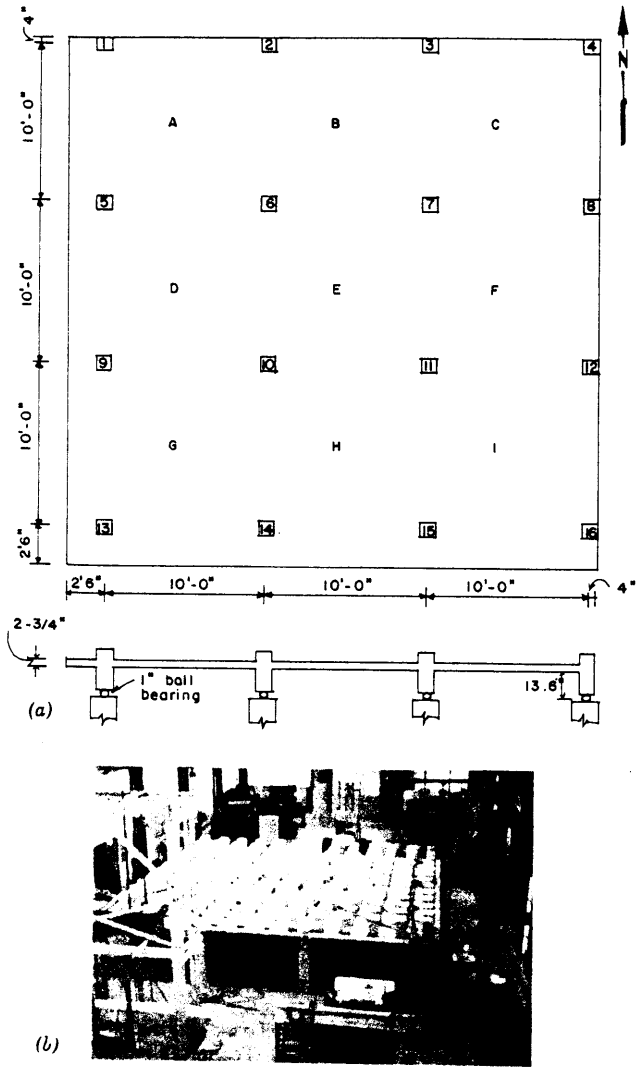

FIG. 1.—Test Slab: (*a*) Plan and Elevation (1 ft = 0.305 m; 1 in. = 25.4 mm); (*b*) Test Slab with Concrete Blocks

50 psf (2,400 N/m^2), partition dead load of 20 psf (1,000 N/m^2), and slab dead load of 103 psf (5,000 N/m^2) [8.25-in. (210-mm) slab thickness] represent typical values for structures of this type. The span/depth ratio was approx

44, which is also representative of the flat plate structures being designed and constructed in the United States. The story height for the prototype structure was 10 ft (3 m).

The design was done for an interior strip of the slab using prismatic rather than *American Concrete Institute (ACI) Code (318-71)* (2) equivalent columns in the equivalent frame analysis. The design was made to balance total slab

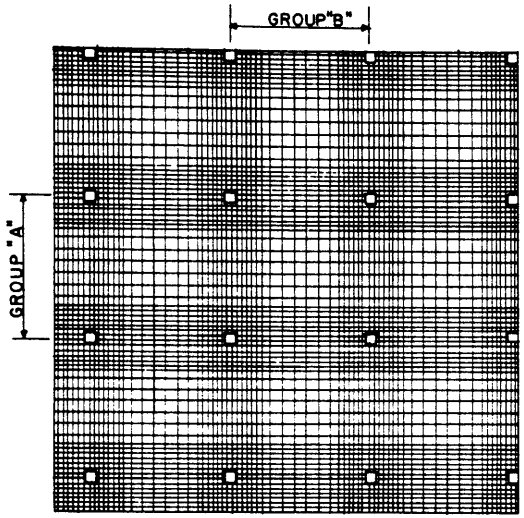

FIG. 2.—Tendon Arrangement for Test Slab (1 in. = 25.4 mm)

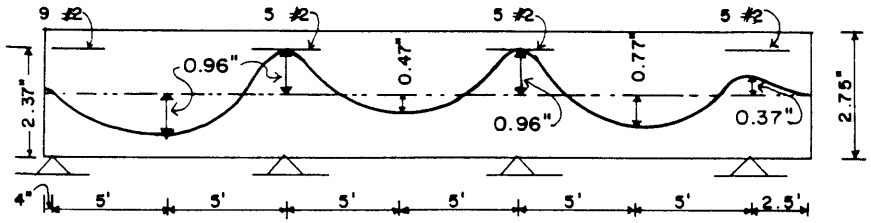

FIG. 3.—Parabolic Drape with Points of Inflection at 1/12 Span (1 ft = 0.305 m; 1 in. = 25.4 mm)

dead load by the unbonded tendons, and the minimum amount of bonded reinforcement recommended by Ref. 12 (0.15% of column strip area) was added to the slab in the immediate column regions. This total reinforcement resulted in actual flexural capacity greater than that required by *ACI Code (318-71)* to resist factored loads. The exterior strip was treated as a half-strip in providing tendons based on load balancing. The column strip at the overhang was provided with the same tendons as were placed at interior column strip. Tendon layout

was symmetrical in the two directions. The same drape of idealized parabolic layout was used for each span, and this layout was closely approximated by the actual profile. Fig. 1 shows the plan view and details of the one-third scale model. The test slab had overall dimensions of 32.5 ft × 32.5 ft (10 m × 10 m) in plan and was nominally 2.75 in. (70 mm) thick [the average actual thickness was 2.9 in. (74 mm)]. Columns 8 in. × 8 in. × 13.6 in. (200 mm × 200 mm × 345 mm) high were spaced 10 ft (3 m) on center in both directions. The stub columns supporting the slab provided the relative flexural stiffness to the slab equivalent to that of columns above and below the slab for the prototype.

The column above the test slab (Fig. 1) provided no flexural resistance, but they induced a stress concentration around the slab-column intersection. The column bases resting on 1-in. (25-mm) diam steel ball bearings which permitted

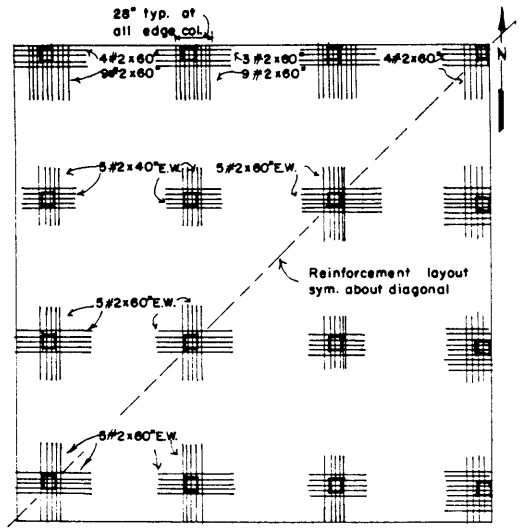

FIG. 4.—Bonded Reinforcement (1 in. = 25.4 mm)

the necessary rotations in all directions at the base of the stub column. However, for the edge columns, the stiffness required for column base restraint against the horizontal movement was not realized at the time of planning and construction of the test slab. From test observations, the as-built column base supplied sufficient resistance to the horizontal thrust (at the bottom of the column) when the slab was loaded with service load; but it was insufficient to resist the horizontal thrust as the failure load was approached. As a result, the test slab, at service load, had the required restraint against the rotation at the edge; but at failure load, the slab had less restraint against rotation than intended.

The slab was post-tensioned with 68 tendons [1/4-in. (6-mm) seven-wire strands] in each direction. The tendons were distributed 70% in the column strip and 30% in the middle strip, as shown in Fig. 2. There were two tendons passing through the column in each direction. The tendon profile was made up of parabolic segments forming a smooth curve, as shown in Fig. 3. The

bonded reinforcement used in the slab at the column areas consisted of five No. 2 (6.3-mm) deformed bars at the interior columns and nine No. 2 (6.3-mm) deformed bars at the edge columns as shown in Fig. 4. Tests of the concrete cylinder indicated strength of f'_{ci} = 3,850 psi (26,500 kN/m²) and f'_c = 4,900

TABLE 1.—Summary of Properties of Prototype and Model Slab

Description (1)	Prototype (2)	True 1/3-scale model slab (3)	As built model slab (4)
Dimension, in feet	97.5 × 97.5	32.5 × 32.5	32.5 × 32.5
Span, in feet	30	10	10
Cantilever, in feet	7.5	2.5	2.5
Thickness, in inches	8.25	2.75	2.90
Number of panels	9	9	9
Number of columns	16	16	16
Column size, in inches	24 × 24	8 × 8	8 × 8
Column height, in inches	120	13.6	13.6
Number of tendons	68 pairs-1/2-in. ϕ		68-1/4-in. ϕ
in each direction	A_{ps} = 20.81 sq in.	A_{ps} = 2.31 sq in.	A_{ps} = 2.44 sq in.
Bonded reinforcement (minimum)	Five No. 6 A_s = 2.2 sq in.	A_s = 0.24 sq in.	Five No. 2 A_s = 0.25 sq in.
Distribution of	70% column	70% column	70% column
tendons to column and middle strips	30% middle	30% middle	30% middle
Percent load balancing	100% DL	100% DL	100% DL
Live load, in pounds per square foot	50	50	50
Partition, in pounds per square foot	20	20	20
Dead load, in pounds per square foot	93.7	34.4	36.2
Concrete strength			
f'_c, in pounds per square inch	4,000	4,000	4,900
f'_{ci}, in pounds per square inch	3,000	3,000	3,850
P/A, in pounds per square inch	325	325	325
Steel strength			
f_y, in pounds per square inch (bonded)	60	60	55
f_{pu}, in pounds per square inch (unbonded)	270	270	250

Note: 1 psi = 6.9 kN/m²; 1 in. = 25.4 mm; 1 lb = 4.45 N.

psi (34,000 kN/m²) although the design was based on f'_c = 4,000 psi (28,000 kN/m²). The steel reinforcement used in the columns of the test structure consisted of No. 3 (9.5-mm diam) deformed bars. The yield stress was 40 ksi

(280 MN/m²), and the modulus of elasticity was 29,000 ksi (200,000 MN/m²). Table 1 shows the properties of a true 1/3-scale model of the prototype along with the properties of the model slab as-built. Slight differences are reflected in the calculations for strength, and the model as built was shown to have 5% more strength than a true 1/3-scale model. In order to satisfy the model

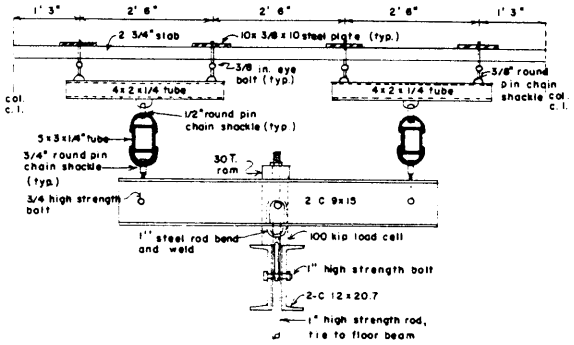

FIG. 5.—Schematic of Main Panel Loading System (Whiffletree) (1 ft = 0.305 m; 1 in. = 25.4 mm)

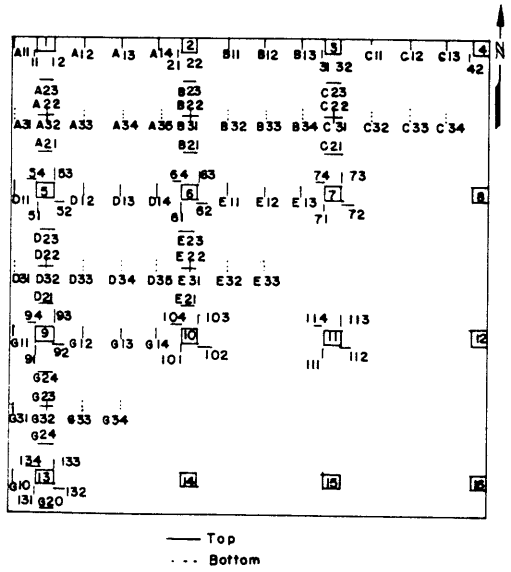

FIG. 6.—Location and Designation of Strain Gages

similitude requirement for dead load, concrete blocks were placed at the load points. The concrete blocks represent the initial part of dead load compensation amount to 58 psf (2,800 N/m²). The remaining part of the dead load compensation, 11 psf (530 N/m²), was obtained from the whiffletree loading system. Total slab dead load (including dead load compensation) was 103 psf (4,900 N/m²).

Loading System.—The slab was loaded by pulling downward with the whiffletree system, producing 16 load points on each main panel and four load points on each span of the overhang as shown in Fig. 5. The whiffletree system for each of the main panels was equipped with one 100-kip (450-kN) load cell and one 30-ton (270-kN) hydraulic ram. The rams for the loading panels were connected to a common manifold that operated from a single pump, and the load cells were connected to the Vidar Data Acquisition Unit. At the pump, the hydraulic pressure was measured with a calibrated pressure gage along with a pressure transducer. The whiffletree system for the overhangs used 10-ton (89-kN) hydraulic rams. The rams were connected to the same pump. Load at the overhangs was measured by the calibrated pressure gage at the pump. No load cells were used at the overhangs. The whiffletree system for a main panel weighed 1.1 kips (5 kN) or equivalent to 11-psf (530-N/m²) load on the slab. This load was used for part of the dead load compensation for both slabs, as indicated earlier. There were altogether 15 whiffletree systems, nine

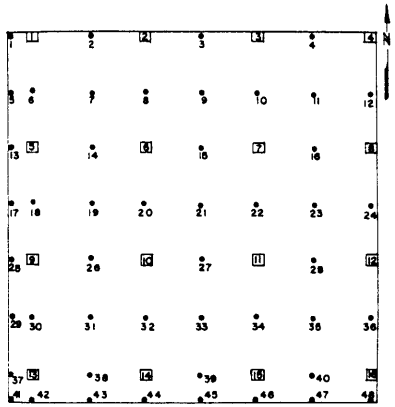

FIG. 7.—Location of Potentiometers

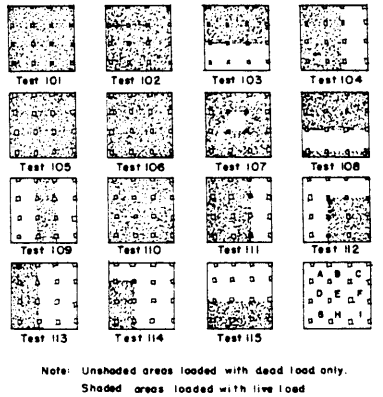

FIG. 8.—Applied Loading Patterns

for the main panels and six for the overhangs. The whiffletree was checked to verify uniform distribution of applied load and adequate strength before installing it onto the slab.

Instrumentation.—The concrete strains were measured by embedding 20-in. (510-mm) long deformed No. 2 (6.3-mm diam) bars equipped with SR-4 strain gages. The locations and designations of these gages are shown in Fig. 6. Note that gages in the vicinity of the columns are at the top of the slab, and these gages were mounted on some of the bars which were provided as bonded reinforcement for the design of the structure (Fig. 4). Four SR-4 strain gages per column were mounted on bars comprising the column reinforcement. The prestressing forces at the holding ends were measured with load cells. Four SR-4 strain gages were mounted directly onto two tendons. These tendons passed alongside columns 9, 10, 11, and 12. The gages were mounted at the high point of the draped tendon layout.

The vertical deflection was measured on the top surface of the slab at 48 locations (Fig. 7) with potentiometers. During each test, the center of panel

deflection was measured with a surveying instrument reading a scale with 1-mm (0.04-in.) accuracy. These scale readings allowed a record of load versus deflection to be plotted during the test to observe significant changes in behavior of each panel. The lead wires from strain gages, load cells, and potentiometer were connected to the Vidar Data Acquisition Unit, which recorded the results on magnetic tape. Much of the data were also typed out through the teletype while recording on the magnetic tape. Data reduction program VIDAR reduced the

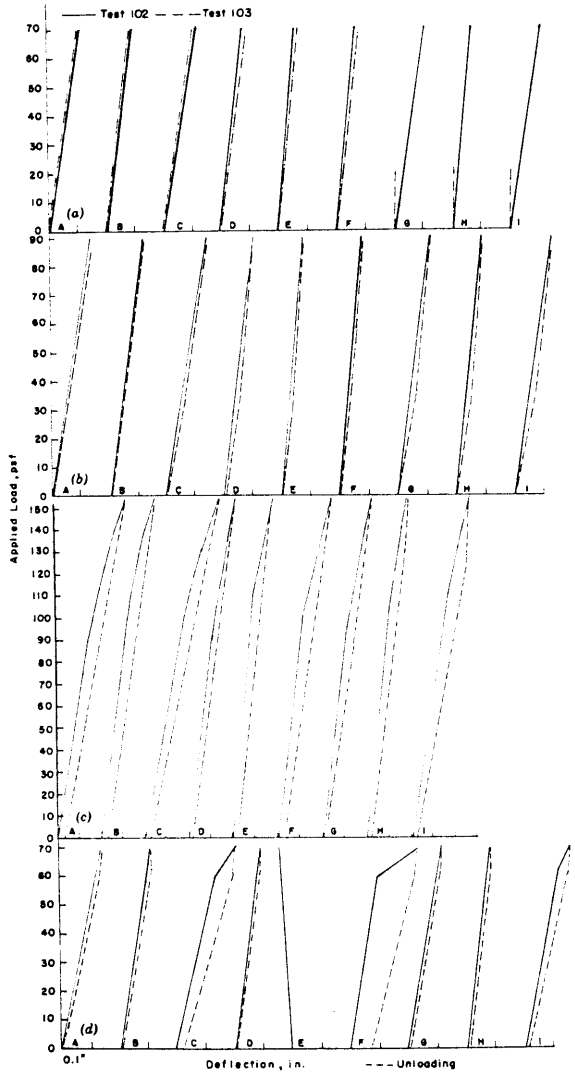

FIG. 9.—Load-Deflection Curves for Test Slab: (*a*) Tests 102 and 103; (*b*) Test 105; (*c*) Test 106; (*d*) Test 107; (*e*) Test 108; (*f*) Test 109; (*g*) Test 110 (1 psf = 47.9 N/m²; 1 in. = 25.4 mm)

magnetic tape record to tabular listings of data and computed loads, strains, and deflections.

Summary of Observed Behavior

The slab was loaded with various loading patterns, ranging from half of the service load through the collapse load. Fig. 8 shows the loading patterns applied to the slab. Test 101 was primarily intended to check the instrumentation of the slab and loading arrangements; therefore, it was loaded only up to 35 psf (1,700 N/m²), or 50% of design service load. It was found that the strain gages, potentiometers, and load cells worked perfectly. The slab behaved elastically. Load-deflection curves at all stations were linear. The deflections recovered completely when the slab was unloaded. There were no signs of cracking or distress anywhere on the slab. Tests 102, 103, and 104 were the first set of tests in which the structure was loaded to service load, 70 psf (3,400 N/m²). The slab behavior was elastic. The load-deflection curves for the loaded panels were linear until the termination of loading, as shown in Fig. 9(*a*). There was no sign of cracking nor yielding of reinforcement. The maximum strain in the bonded reinforcement was recorded at the northeast corner of column 7 (strain gage No. 73 of Fig. 6) as 243 μ in./in. [7-ksi stress (48 MN/m²)].

The first cracking load test was Test 105 [Fig. 9(*b*)]. The slab was loaded with increasing increments of 5 psf (240 N/m²) until the first crack was observed. The slab was examined for cracks at each load increment after the load previously applied had been exceeded [70 psf (3,400 N/m²)]. The first cracking was observed at the face of interior columns 6, 7, and 11. The load deflection curves for

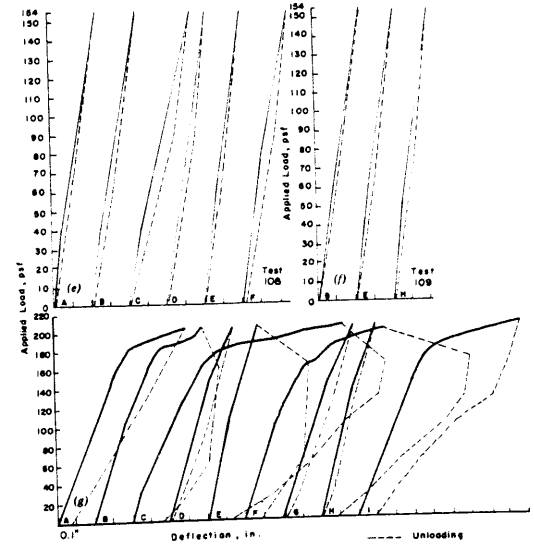

FIG. 9.—*Continued*

the centers of panels are linear until the termination of loading. The maximum deflection was 0.15 in. (3.8 mm) at panel C. The maximum strain in the bonded

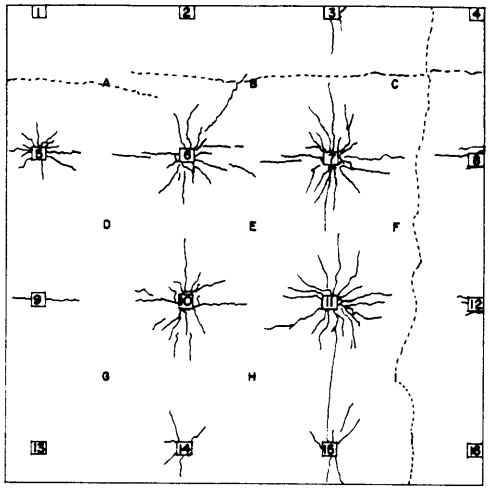

FIG. 10.—Crack Pattern on Test Slab after Test 110

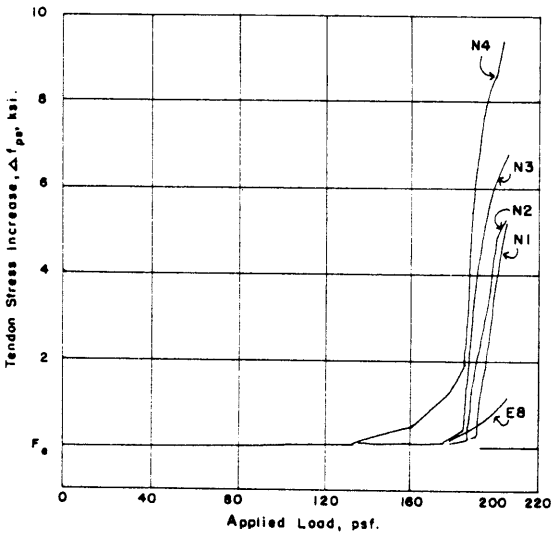

FIG. 11.—Measured Tendon Stress Increase during Test 110 (Load Cells at Holding Ends) (1 psi = 6.9 kN/m²; 1 psf = 47.9 N/m²)

reinforcement was recorded at the northeast corner of column 7 (strain gage No. 73) as 374 μ in./in. [11-ksi stress (76 MN/m²)].

There were extensive cracks around the four interior columns under the factored load ($1.4D + 1.7L$) of Test 106. No bottom cracks were observed under this

load case. The deflections at every station were proportional to the applied loads until about 90 psf (4,300 N/m²). After 90 psf, the slab exhibited a nonlinear load-deflection behavior due to loss of stiffness of the slab in the column areas [Fig. 9(*c*)]. The maximum deflection under factored service load was 0.35 in. (8.9 mm) observed at panel C. The tendon stress changed insignificantly. No yielding of bonded reinforcement was measured at factored load. The test to simulate loss of prestress in the interior panels was Test 107. The tendons in groups "A" and "B" (see Fig. 2) were completely destressed. This resulted in a total loss of prestress in panel E and one-way slab action in panels B, D, F, and H. The slab carried the service load, 70 psf (3,350 N/m²), on all exterior panels without serious damage, although the slab had some flexural cracks which resulted from the previous tests. A bottom crack formed in panel F which caused nonlinearality of load-deflection response in panel F and in the adjacent panels C and I [Fig. 9(*d*)]. The maximum deflection at the center of panel F was 0.24 in. (6 mm). The tendons were retensioned to their original stress upon the completion of Test 107.

The pattern loading under factored load (Tests 108 and 109) produced maximum negative and positive moment in the slab. The pattern load did not change the crack pattern on the slab. The top cracks near the columns were slightly lengthened and widened under load, but no new bottom cracking was observed. The slab load-deflection response was only slightly nonlinear until the conclusion of these tests [Figs. 9(*e*) and 9(*f*)]. No significant change in tendon stress was observed.

In the test to failure (Test 110), the slab started to behave nonlinearly in panels C, F, and I when the applied load started [Fig. 9(*g*)]. The early nonlinearity of load-deflection curves was caused by the top and bottom flexural cracks of previous tests. As the load increased, very large deflection was observed visually in panels C, F, and I which had bottom cracking at midspan from Test 107. After a load of 190 psf (9,000 N/m²), the slab was still capable of carrying more load, but deflection was increasing much more rapidly than previously for several panels (especially panels C, F, and I) as shown in Fig. 9(*g*). When the applied load reached 205 psf (9,800 N/m²), punching shear failure occurred suddenly at the interior column No. 7. As soon as the punching shear failure occurred, the pressure in the hydraulic system was relieved, and the load decreased to about 180 psf (8,600 N/m²). Deflection increased slightly at the middle of surrounding panels due to the shear displacement even though the load decreased. The vertical displacement of the slab at the faces of column 7 after the punching shear failure was about 0.75 in. (19 mm) Fig. 10 shows the crack pattern at the conclusion of Test 110. The punching shear tests (Tests 111, 112, 113, 114, and 115) were arranged to study the shear capacity of the slab only. Therefore, the flexural behavior under load was not observed. The measured loads from the hydraulic pressure times the tributary areas gave an estimate of shear capacity for the slab which was relatively consistent from one column to another.

Measured Tendon Stress.—Fig. 11 shows the relationship between the increase in stress in the unbonded prestressing strands and the applied load. The tendon stress increase was observed at the outside edge, where load cells recorded the change in holding force. The curves in Fig. 11 show that the stress remained at the initial effective stress level until very near the failure load. The stress

in the tendons increased sharply as the applied load exceeds 180 psf (8,600 N/m^2) which is the load level corresponding to rapid increase in deflection

TABLE 2.—Comparison of Tendon Stresses for Test 110, in kips per square inch

Instrument number (1)	Measured tendon stress increment, Δf_{ps} (2)	Corrected tendon stress increment[a], Δf (3)	f_{ps} (test) $= f_{se} + \Delta f$ (4)	f_{ps} (ACI) (5)	f_{ps} (test)/ f_{ps} (ACI) (6)
N1	5.2	5.5	150	173	0.87
N2	5.3	5.8	150	173	0.87
N3	6.7	7.2	151	173	0.87
N4	9.5	10.0	154	173	0.89
ST-1	21.0		165	173	0.95
ST-4	25.4		169	173	0.98

[a]Estimated by using *ACI 318-71* equation.
Note: Effective tendon stress (f_{se}) = 144 ksi; 1 ksi = 6.9 MN/m^2.

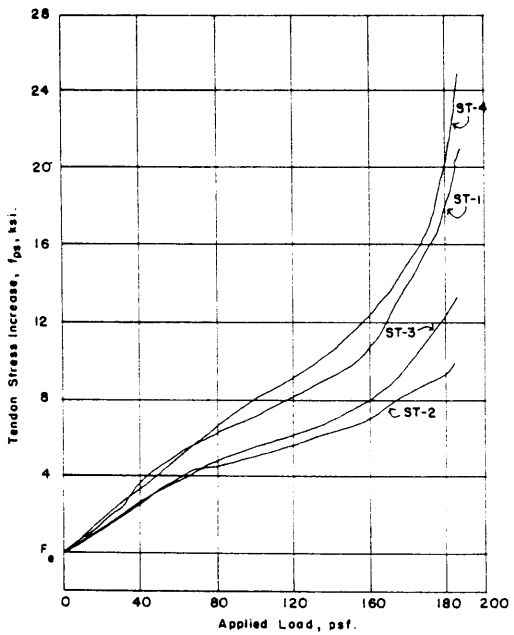

FIG. 12.—Measured Tendon Stress Increase during Test 110 (Strain Gages on Tendons) (1 psi = 6.9 kN/m²; 1 psf = 47.9 N/m²)

for the three panels at the north edge [Fig. 9(g)]. The bottom crack in panels A, B, and C formed at this load. The final measured tendon stress increase varied from 5.2 ksi (36 MN/m^2)–9.5 ksi (66 MN/m^2) depending upon the locations

of load cells and the deflection of the slab strip that the tendon passed through.

The stresses plotted in Fig. 12 were measured directly by means of strain gages on the tendons at a point of peak moment adjacent to the interior columns 9, 10, 11, and 12. Since the slab was cracked at the interior column region prior to Test 110, Fig. 12 shows a faster rate of tendon stress increase than Fig. 11. The final measured tendon stresses of Fig. 12 from tendon strain measurement at interior supports were larger than those of Fig. 11 measured by load cells at the edge of the slab.

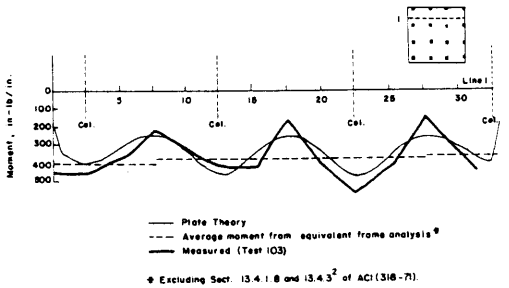

FIG. 13.—Comparison of Measured Positive Moments Across Panels A, B, and C with Theoretical Moments (1 in.-lb/in. = 4.45 N·mm/mm; 1 ft = 0.305 m)

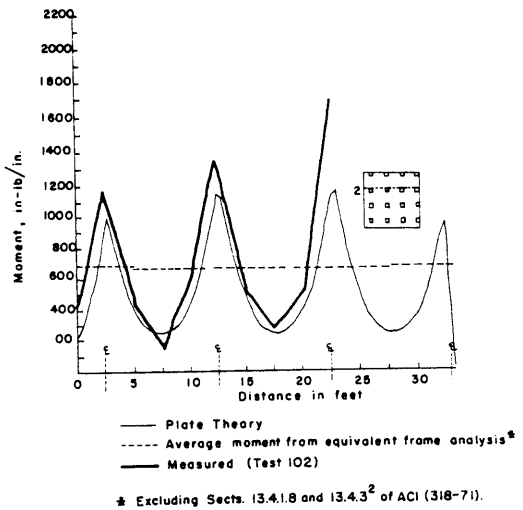

FIG. 14.—Comparison of Measured Negative Moments Across Columns 5, 6, 7, and 8 with Theoretical Moments (1 in.-lb/in. = 4.45 N·mm/mm; 1 ft = 0.305 m)

Table 2 shows the tendon stress increases measured by both holding end load cells and the strain gages on the tendons. The estimated tendon stresses at the negative moment yield lines (first interior column line) have been included in Table 2. The stress was estimated by using the Ref. 2 friction loss equation (No. 18-1), in order to correct for the fact that the load cells were located

at the edge of the slab. By investigating Table 2, it is obvious that the estimated stress at the negative moment yield line is lower on the basis of corrected load cell data than the measured stress based on strain gage data from strains ST-1 and ST-4. The difference was due to the locally high tendon stress increase in the region of high tendon curvature near the yield lines.

Measured Moments.—The studies of moment distribution across the section were based upon the strains measured from the embedded No. 2 (6.3 mm diam) deformed bars at the locations, as shown in Fig. 6. The concrete strains at the level of bar were assumed to be equal to the measured steel strains. The strains were converted to slab moments per unit width for each strain gage location and were assumed to be representative of the strains in a strip of

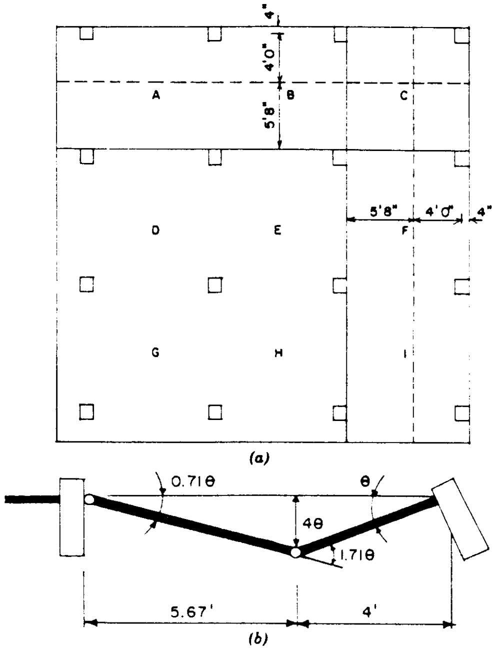

FIG. 15.—Yield Line Pattern of Test Slab: (*a*) Plan View; (*b*) Collapse Mechanism (1 ft = 0.305 m; 1 in. = 25.4 mm)

the slab 1/2 in. from the gage on each side. Thus, the moments for figures in this section are given in units of inch-pounds per inch. The strains were assumed to vary linearly between gages. The measured strains in concrete were related to bending moment by

$$M = \frac{\epsilon E_c I}{c} \quad \ldots \quad (1)$$

in which M = bending moment; ϵ = concrete strain (measured steel strain); E_c = modulus of elasticity of concrete; c = distance from neutral axis; and I = moment of inertia of unit width of slab.

The conversion of the measured strain to moment involves the flexural stiffness, $E_c I$, for the slab as shown in the preceding equation. The effective $E_c I$ =

TABLE 3.—Column Load at Punching Shear Failure

		Calculated Column Load, in kips	
Test (1)	Column (2)	Measured column steel strain (3)	Failure mechanism reaction (4)
110	7	34.3	33.8
111	6	35.3	36.4
111	10	36.5	37
112	11	—	28.1
113	5	28.9	26.4
114	9	27.1	25.3
115	15	—	25.9

Note: 1 kip = 4.45 kN.

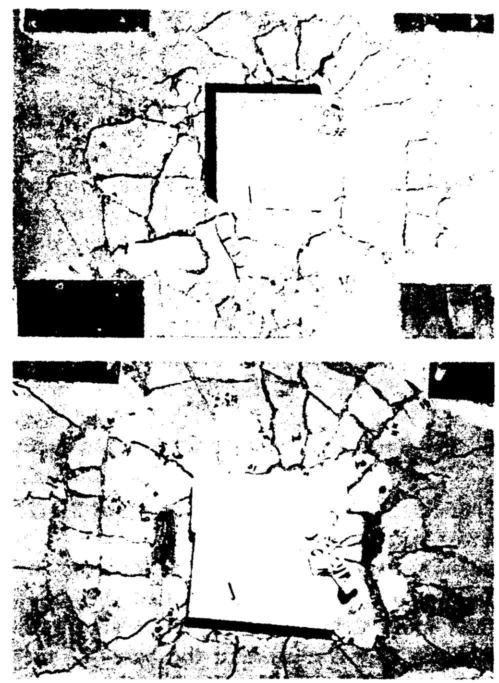

FIG. 16.—Photographs of Punching Shear Failure (Typical)

5.8×10^6 lb-sq in./in. (660 MN-mm^2/mm) was used in computing the measured moments. The effective $E_c I$ was determined by comparing the measured deflections of the test slab to deflections calculated from elastic plate theory

using the computer program developed by Panak (10).

The moments per unit width calculated from the measured strains were plotted in Figs. 13 and 14. The moments were based upon the applied service loads for the slabs. For the purpose of comparison, the moments calculated from the equivalent frame method based upon Ref. 2 and the moments solved by the elastic plate theory using a discrete element method are presented in Figs. 13 and 14. The comparison of the magnitude and distribution of calculated theoretical moments by plate theory with those obtained experimentally at the positive moment area indicates fairly good agreement in both the column strip and middle strip regions of the slab. Discrepancy was found when comparing the positive moment calculated from the frame method, as shown in Fig. 13, with the measured moment that was high at the column lines. The measured moments reflect the trend of variation obtained from plate theory while the frame analysis method with the exclusion [as recommended by ACI-ASCE

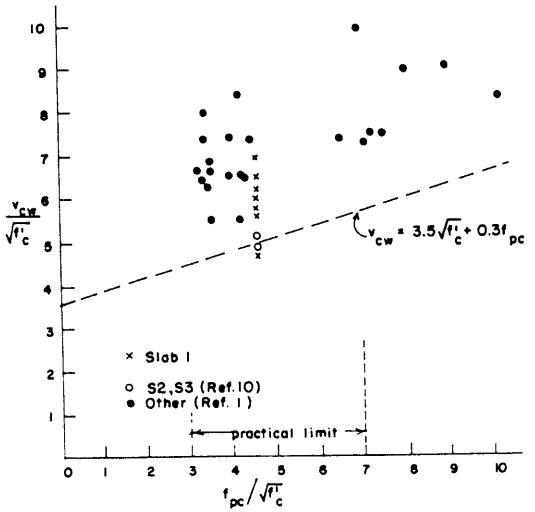

FIG. 17.—Shear Test Data Versus Ref. 12 Equation

Committee 423(12)] of Section 13.4.3 of *ACI Code (318-71)* (2) provides uniform average moment across a section.

Flexural Strength.—Due to the relaxation of the column base as the load was approaching failure load, it was realized that the rotation of the slab at the edge column was more than would be observed for the slab with good control of column bases. It was clear that the bases of the exterior columns moved outward. The prediction of the ultimate flexural load was based on yield-line theory for the slab with zero restraint at the edge for this reason. The tendon stress was obtained from Eq. 18-4 of Ref. 2. The possible yield lines involve only the flexural failure of the slab at the exterior panels as shown in Fig. 15. The calculated load of 309 psf (14,800 N/m^2) shown in Appendix I is in very good agreement with the total load at failure, 308 psf (14,700 N/m^2) which is the sum of applied load, 205 psf (9,800 N/m^2), concrete blocks, 58

psf (2,800 N/m^2), whiffletree, 11 psf (530 N/m^2), and slab own weight, 34 psf (1,600 N/m^2).

Slab Shear Strength.—Fig. 16 shows the photographs of the cracking at punching shear failure of the test slab. The shear failure occurred only at the interior columns. Table 3 shows the column loads from punching shear tests. The data from strain gages on the column reinforcement provided one means of calculating the column load at failure. The failure mechanism developed in flexure prior to the punching shear failure in these tests. Calculation of the reaction at the column consistent with the flexural failure mechanism gives another prediction of the column load at punching shear failure. All of the tests from Test 110–Test 115 exhibited a sudden and complete punching failure of the column with extensive cracks around the columns. As the column punched through the slab, it pushed out a plug of concrete having the shape of a truncated pyramid. The inclined surfaces of the pyramid made an angle of 19°–21° with the top surface of the slab. The base of the pyramid at the top of the slab was approx 2 ft square (0.6 m square).

Fig. 17 shows the plot of shear test data obtained from the test slab along with the values obtained from test results by others. The comparison of test results with the equation recommended by Ref. 12 shows that the Committee 423 equation predicts the slab shear strength with safety.

Conclusions

From a review and analysis of this study, the following conclusions can be drawn:

1. Bonded reinforcement providing 0.15% of the cross-sectional area of the column strip as suggested by Ref. 12 effectively controlled the distribution of flexural cracks and contributed to the ultimate load capacity of the slab. Placement of bonded reinforcement in the prestressed slab is as important as the amount. The placement of minimum bonded reinforcement as top steel in the immediate column vicinity provided excellent performance.
2. The prototype slab was designed by using frame analysis along with the distribution of tendons into column and middle strip (70%–30%) and the allowable concrete stresses suggested by Ref. 12. The one-third scale model slab behaved satisfactorily at service load and carried higher flexural ultimate load than the *ACI Code (318-71)* factored load.
3. Measured tendon stresses at ultimate load were 2%–13% below the predicted ultimate stress from the *ACI Code (318-71)* equation. The steel stress in the unbonded tendons increased insignificantly until large deflection developed as ultimate strength was approached.
4. Shear strength of the slab is affected by the concrete compressive stress, amount of bonded reinforcement, and the tendon arrangement, with the concrete compressive stress, P/A, probably influencing the shear capacity most. The shear capacity calculated by the equation of Ref. 12 gives reasonable results for the test slab which had 70% of the tendons in the column strip. The slab shear strength exceeded the strength recommended by Ref. 12.

Design Recommendations

1. Bonded reinforcement at the peak negative moment areas around columns

should always be used. The minimum reinforcement area, 0.15% of the cross-sectional area of the column strip, is adequate to control overload cracking. The bonded reinforcement should be placed within a distance $1.5t$ from faces of the column (t = thickness).

2. The equivalent frame analysis of *ACI (318-71)*, Chap. 13 should be used in the design of prestressed flat plates with unbonded tendons. Measured moments from this study justify the equivalent frame analysis to obtain the average moment at the various critical sections for design. The equivalent frame analysis will lead to higher design moments for the slab at the first interior column and lower moments at the exterior column than would result from prismatic frame analysis. Provision of strength on this basis will lessen the moment capacity provided at the exterior column and place more flexural reinforcement at the interior sections, where it is certain to be fully effective at ultimate.

3. The distribution of tendons with 70% in column strip and 30% in middle strip in each direction suggested by Ref. 12 will provide excellent slab performance.

4. As many tendons in each direction as practical should pass through the column. The exterior column benefits from localized anchorage of prestress at the column, increasing the P/A stress above the average value for the panel. This higher P/A increases the flexural cracking and enhances the shear strength.

Acknowledgment

The experimental work reported in this study was performed at the Civil Engineering Structures Laboratory of the University of Texas, Austin, Tex. This work was sponsored principally by the Post-Tensioning Division of the Prestressed Concrete Institute (now the Post-Tensioning Institute), and their support is acknowledged. Partial financial support from the Bureau of Engineering Research of the University of Texas at Austin and the Reinforced Concrete Research Council is also acknowledged.

Appendix I.—Calculation of Ultimate Load

1. Referring to Fig. 15 for yield line pattern: Avg t = 2.9 in., f'_c = 4,900 psi.

2. Calculate stress in tendon at design load (Ref. 2, Eq. 18-4): A_{ps} = 20 × 0.036 = 0.72 sq in. (4.7 cm²); $f_{ps} = f_{se} + 10{,}000 + f'_c/100_{\rho_p}$; f_{ps} = 144 + 10 + 4.9/100 × 0.00257 = 173 ksi (1,200 MN/m²).

3. Calculate reinforcement index ω_p: $\omega_p = A_{ps}f_{ps}/bdf'_c + A_s f_y/bdf'_c$; ω_p = (0.72 × 173/120 × 2.375 × 4.9) + (0.25 × 55/120 × 2.375 × 4.9); ω_p = 0.099 < 0.3 O.K.

4. Calculate moments M_u: a_1 = (0.72 × 173 + 0.25 × 55)/(0.85 × 120 × 4.9) = 0.276 in. (7 mm); M_{u1} = 138(2.335 − 0.276/2) = 303.0 kip-in.; M_{u1} = 25.3 kip-ft; a_2 = 0.72 × 173/(0.85 × 120 × 4.9) = 0.249 in.; M_{u2} = 124.5(2.485 − 0.249/2) = 294 kip-in. = 24.5 kip-ft.

5. Energy input = 0.5 × 9.67 × 4θxw_u kip-ft.

6. Work at yield line = 24.5 × 1.71θ + 25.3 × 0.71θ kip-ft. = 59.8θ kip-ft.

7. Equating energy input to work at yield line: w_u = 3.09 kip-ft.; w_u = 309 psf (14,800 N/m²).

Appendix II.—References

1. Brotchie, J. F., and Beresford, F. D., "Experimental Study of a Prestressed Concrete Flat Plate Structure," *Paper No. 2298*, Division of Building Research, Commonwealth Scientific and Industrial Research Organization, Melbourne, Australia, May, 1967.
2. "Building Code Requirements for Reinforced Concrete," *ACI 318-71*, American Concrete Institute, Detroit, Mich., 1971.
3. Gamble, W. L., "An Experimental Investigation of the Strength and Behavior of a Prestressed Concrete Flat Plate," *Report T8, 0-9*, Division of Building Research, Commonwealth Scientific and Industrial Research Organization, Melbourne, Australia, 1964.
4. Gerber, L. L., and Burns, N. H., "Ultimate Strength Tests of Post-Tensioned Flat Plates," *Prestressed Concrete Institute Journal*, Vol. 16, No. 6, Nov.-Dec., 1971.
5. Grow, J. B., and Vanderbilt, M. D., "A Study of the Shear Strength of Lightweight Prestressed Concrete Flat Plates," *Structural Research Report No. 3*, Civil Engineering Department, Colorado State University, Fort Collins, Colo.; also in *Prestressed Concrete Institute Journal*, Vol. 12, No. 4, Aug., 1967.
6. Hemakom, R., "Strength and Behavior of Post-Tensioned Flat Plates with Unbonded Tendons," thesis presented to the University of Texas, at Austin, Tex., in 1975, in partial fulfillment of the requirements for the degree of Doctor of Philosophy.
7. Lin, T. Y., Scordelis, A. C., and Itaya, R., "Behavior of a Continuous Concrete Slab Prestressed in Two Directions," Institute of Engineering Research, University of California, Berkeley, Calif., Aug., 1958; also in *American Concrete Institute Journal*, Dec., 1959.
8. Lin, T. Y., Scordelis, A. C., and May, H. R., "Shearing Strength of Prestressed Concrete Lift Slabs," *American Concrete Institute Journal*, Vol. 55, No. 4, Oct., 1958.
9. Lu, F., "Strength and Behavior of a Nine Bay Continuous Concrete Slab Prestressed in Two Directions," University of Canterbury, Christchurch, New Zealand, Mar., 1966.
10. Panak, J. J., "A Discrete Element Method of Multiple-Loading Analysis for Two-Way Bridge Floor Slabs," thesis presented to the University of Texas, at Austin, Tex., in 1968, in partial fulfillment of the requirements for the degree of Master of Science.
11. Smith, S. W., and Burns, N. H., "Post-Tensioned Flat Plate to Column Connection Behavior," *Prestressed Concrete Institute Journal*, Vol. 19, No. 3, May-June, 1974.
12. "Tentative Recommendations for Prestressed Concrete Flat Plates," by the American Concrete Institute-ASCE Joint Committee 423—Prestressed Concrete, *American Concrete Institute Journal*, Vol. 71, No. 2, Feb., 1974.